Supporting Information

Maloney et al. 10.1073/pnas.1203126109

SI Materials and Methods

Cell Culture and Somatic Cell Hybrid Construction. Human lymphoblastoid lines were cultured in RPMI 1640 medium (Invitrogen). Human fibrosarcoma cell line HT1080 and the primary human dermal fibroblast cell line were cultured in Minimum Essential Medium Alpha (Invitrogen). Human colorectal carcinoma line HCT116 was grown in McCoy's 5A medium (Invitrogen). All media were supplemented with 1× Antibiotic-Antimycotic (Gibco, Invitrogen). Mouse–human somatic cell hybrid lines containing a single *Homo sapiens* chromosome 17 (HSA17) were constructed by polyethylene glycol fusion of human cells with mouse thymidine kinase-deficient L cells (1). Single-cell clones were isolated after 14 d using hypoxanthine-aminopterin-thymidine selection, expanded for 1–2 wk, and examined using FISH with chromosome-painting probes and a probe specific for alpha-satellite array D17Z1 on HSA17. Clones containing a single HSA17 in >90% of cells were selected for further study.

Resizing and Retrofitting BAC Constructs. RP11-285M22 was resized from ~158 kb to ~61 kb by removing a monomeric alpha satellite between two PmlI sites. The resulting vector, 285M22Pml1, contained eight units of HOR D17Z1-B DNA. BACs were retrofitted with selectable markers (KAN/NEO or AMP/NEO) using the EZ-Tn5 pMOD-2 < MCS > Transposon Construction Vector (Epicentre Biotechnologies). The Kan/Neo resistance cassette was PCR amplified from EGFP-c1 template by PCR (Table S2). Primers were designed with overhangs containing EcoRI and KpnI recognition sites, respectively, to allow cloning into the polylinker of pMOD-2 < MCS>. Transposition reactions were carried out according to the instructions of the manufacturer of EZ-Tn5 Tranposase (Epicentre). Two microliters of the transposition reaction were electroporated into TransforMax EC100 Electrocompetent *Escherichia coli* (Epicentre). To avoid interruptions in alpha-satellite DNA, only constructs in which the Tn5 cassette inserted into the vector backbone were selected for further use. These constructs were detected by PCR using primers FW1/RV1 and FW2/RV2 to detect a 2-kb increase in construct size. Increased vector size also was verified by pulsed-field gel electrophoresis, and constructs were sequenced to verify the entry of the Tn5K/N cassette into vector sequences only.

In a second approach, single-step in vivo site-specific homologous recombination was used to introduce a neomycin cassette contained on the construct pRetroES into D17Z1 or D17Z1-B BACs. pRetroES contains a tac-GST-*lox*P-cre fusion gene that upon transformation into competent BAC strains recombines into the *lox*P site on the BAC (2). After integration, the *cre* gene is disrupted at the *lox*P site and inactivated. The pBACe3.6 has a wild-type *lox*P and a mutated form, *lox*511; the latter recombines inefficiently. Recombinant colonies were screened by PCR (Table S2) to verify pRetroES to determine *lox*P or *lox*511 integration (2). Only retrofitted BACs containing a single pRetroES insertion were selected for transfection.

Transfection of HT1080 Cells with BACs Containing Alpha-Satellite DNA. The HT1080 cell line (CCL-121; ATCC) was cultured in Minimum Essential Medium Alpha with 10% FBS SH30071.03; (HyClone) and 1% (vol/vol) penicillin and streptomycin or 1× Antibiotic-Antimycotic. HT1080 cells were transfected using Fugene 6 (Roche) according to the manufacturer's instructions using a 3:2 ratio of Fugene DNA transfection reagent:DNA complex. Stable clones were identified after 10–14 d on the basis of their resistance to 600 μL/mL G418 Sulfate (Mediatech Cellgro). Single colonies were expanded to generate clonal lines for further analysis.

FISH on Fixed Metaphase Chromosomes and Extended Chromatin Fibers. Exponentially growing cultures were arrested in metaphase by treating cells with 10 ug/mL colcemid (Invitrogen) for 30–35 min. To introduce stretching of the centromere regions of metaphase chromosomes, 10 ug/mL of ethidium bromide (American Bioanalytical) was added to cultures 30 min before or concurrently with the addition of colcemid. Stretched chromatin fibers were prepared using published methods (3, 4). FISH was performed as previously described (4, 5). Plasmid probes specific for D17Z1 (p17H8) (6) and D17Z1-B (p2.5–3) (both gifts of Huntington Willard, Duke University, Durham, NC) were labeled by standard nick translation with biotin 16-dUTP, digoxygenin 11-dUTP, or Alexa Fluor 488-dUTP or 568-dUTP (Molecular Probes, Invitrogen). To prevent cross-hybridization between D17Z1 and D17Z1-B probes, 68% (vol/vol) hybridization [68% (vol/vol) deionized formamide, 10% (vol/vol) dextran sulfate, 1% (vol/vol) Tween-20, 2× SSC] and washing buffers [68% (vol/vol) formamide, 2× SSC, 0.1% Tween-20] were used.

Combined Immunofluorescence and FISH. Unfixed human metaphase chromosomes were prepared as previously described (7). Cells were arrested in metaphase using colcemid in the presence of ethidium bromide to limit condensation of DNA. Extended chromatin fibers were generated as described (4). CENP-A antibodies included commercially available monoclonal antibodies to human CENP-A (1:400) (13939; Abcam) and custom rabbit polyclonal antibodies to mouse Cenp-A (1:400) (AP601; QCB/Biosource).

Microscopy and Image Analysis. All images were captured using an Olympus IX71 inverted microscope connected to the Deltavision RT deconvolution imaging system (Applied Precision) and processed with the Deltavision SoftWoRx Resolve3D program. Images were deconvolved using the conservative algorithm with 10 iterations and viewed using the quick projection option. Chromatin fibers often extended through multiple fields of view that were collected as separated images and merged using the Stitch Image function in SoftWoRx (4). Metaphases were scored for colocalization of D17Z1 or D17Z1-B with CENP-A using visual and semiquantitative approaches. Lateral and axial line scans were drawn through the centromere with a custom histogram-line plot macro in the IPLab software program (Scanalytics) (8) that generated graphs of pixel distance vs. signal intensity. The peaks of each curve in the graph (D17Z1 in red, D17Z1-B in green, and CENP-A in blue) were measured, along with the start and end pixel values of the region of the curve above 50 fluorescence units. The proportion of CENP-A pixels (above 50 fluorescent units) that overlapped with the D17Z1 and D17Z1-B arrays were calculated and expressed as a percentage.

Chromatin Isolation and ChIP Followed by Semiquantitative PCR. Native chromatin containing oligonucleosomes was prepared by micrococcal nuclease digestion as previously described (3, 4, 9). Initially, 25 μg of chromatin was incubated with 5–10 μg of monoclonal human CENP-A antibodies (ab13939; Abcam), 5 μg of polyclonal antibodies recognizing mouse Cenp-A (AP601) and 100 uL protein G or A beads. One microliter of immunoprecipitation product (IP) was used in each PCR that was performed in duplicate. PCR primers were specific to D17Z1 (10, 11), D17Z1-B (Table S2), and a control site on proximal 17p (D17S2040). Relative enrichment (RE) for CENP-A at each position (query) was calculated using $RE = [(IP/Mock)/(Input/Mock)]_{query}/[(IP/Mock)/(Input/Mock)]_{normalization}$. RE values from each ChIP reaction were averaged.

1. Willard HF, Greig GM, Powers VE, Waye JS (1987) Molecular organization and haplotype analysis of centromeric DNA from human chromosome 17: Implications for linkage in neurofibromatosis. *Genomics* 1:368–373.
2. Wang Z, Engler P, Longacre A, Storb U (2001) An efficient method for high-fidelity BAC/PAC retrofitting with a selectable marker for mammalian cell transfection. *Genome Res* 11:137–142.
3. Lam AL, Boivin CD, Bonney CF, Rudd MK, Sullivan BA (2006) Human centromeric chromatin is a dynamic chromosomal domain that can spread over noncentromeric DNA. *Proc Natl Acad Sci USA* 103:4186–4191.
4. Sullivan LL, Boivin CD, Mravinac B, Song IY, Sullivan BA (2011) Genomic size of CENP-A domain is proportional to total alpha satellite array size at human centromeres and expands in cancer cells. *Chromosome Res* 19:457–470.
5. Stimpson KM, et al. (2010) Telomere disruption results in non-random formation of de novo dicentric chromosomes involving acrocentric human chromosomes. *PLoS Genet* 6:e1001061.
6. Waye JS, Willard HF (1986) Structure, organization, and sequence of alpha satellite DNA from human chromosome 17: Evidence for evolution by unequal crossing-over and an ancestral pentamer repeat shared with the human X chromosome. *Mol Cell Biol* 6:3156–3165.
7. Sullivan BA, Karpen GH (2004) Centromeric chromatin exhibits a histone modification pattern that is distinct from both euchromatin and heterochromatin. *Nat Struct Mol Biol* 11:1076–1083.
8. Blower MD, Sullivan BA, Karpen GH (2002) Conserved organization of centromeric chromatin in flies and humans. *Dev Cell* 2:319–330.
9. Mravinac B, et al. (2009) Histone modifications within the human X centromere region. *PLoS ONE* 4:e6602.
10. Warburton PE, Greig GM, Haaf T, Willard HF (1991) PCR amplification of chromosome-specific alpha satellite DNA: Definition of centromeric STS markers and polymorphic analysis. *Genomics* 11:324–333.
11. Yang DY, Eng B, Waye JS, Dudar JC, Saunders SR (1998) Technical note: Improved DNA extraction from ancient bones using silica-based spin columns. *Am J Phys Anthropol* 105:539–543.

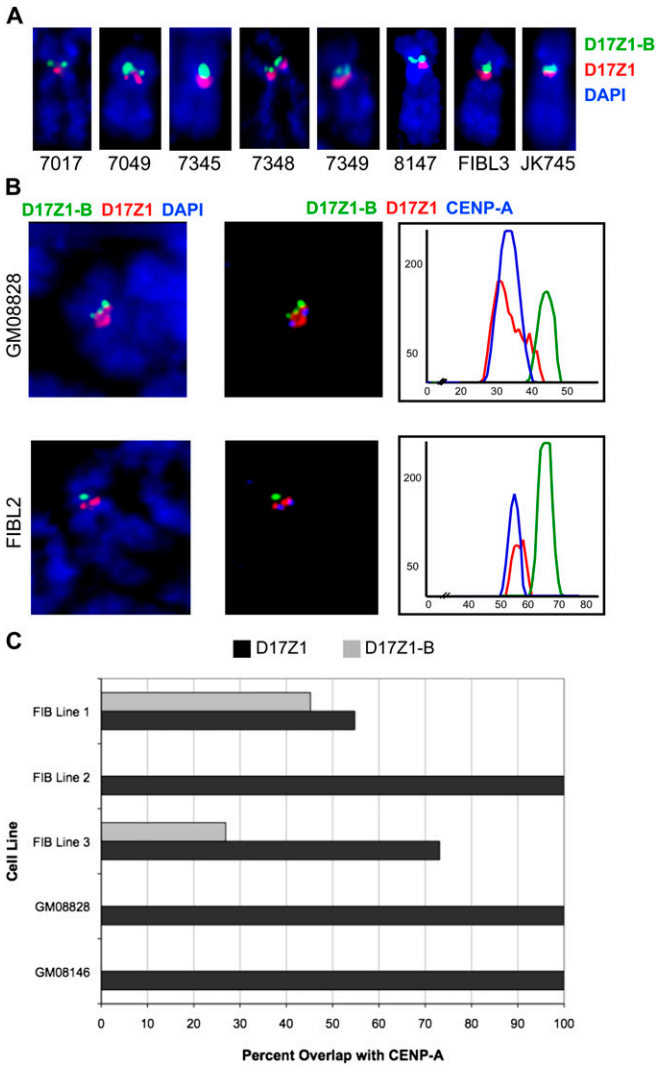

Fig. S1. Semiquantitative immunofluorescence-FISH approach for assigning the CENP-A location on HSA17 in diploid human cell lines. (*A*) Both HSA17s in each cell line were examined for orientation of D17Z1 (red) and D17Z1-B (green) using two-color FISH. In all cases, D17Z1-B was located on the short arm side of the centromere, as shown in representative HSA17 images from eight different cell lines. (*B*) Two examples illustrating how the custom computer script was used to assign the CENP-A location on HSA17s from lines GM08828A and FIBL2. Immunostaining for CENP-A (blue) followed by FISH with probes for D17Z1 (red) and D17Z1-B (green) was performed. Each image was analyzed using a custom line plot script in which a line was drawn down each chromatid of the chromosome and the fluorescence units were plotted along chromosome length. The overlap of the blue curve (CENP-A) with either D17Z1 or D17Z1-B was scored. (*C*) Graph showing the percentage of individual HSA17s that showed CENP-A at D17Z1 and D17Z1-B. Cell lines in which CENP-A was located at D17Z1 in 100% of the cells analyzed showed this localization on both homologs. Cell lines such as FIBL1 and FIBL3 showed approximately 50% D17Z1 and 50% D17Z1-B localization, meaning that CENP-A was located at different HOR repeat arrays on the two HSA17 homologs.

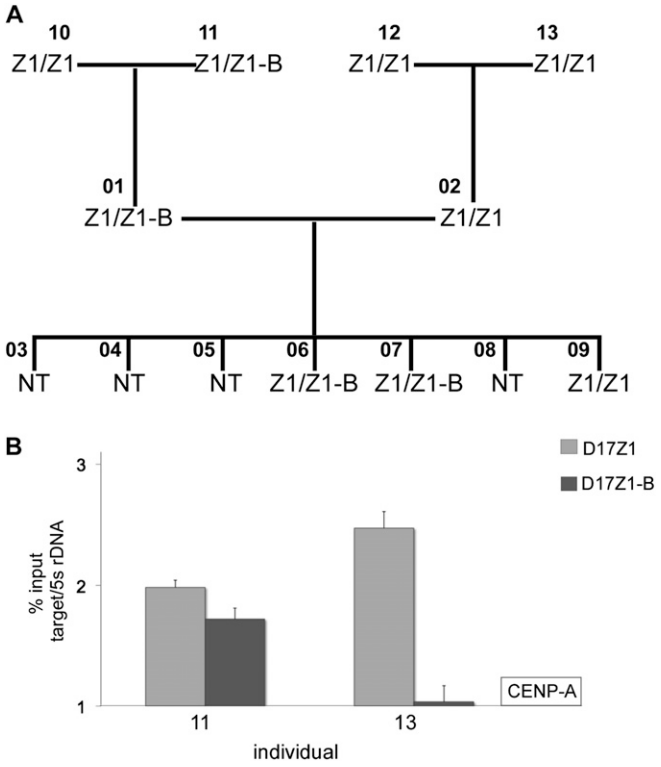

Fig. S2. Variable CENP-A location in humans and stable transmission through meiosis. (*A*) Analysis of Centre du Etude Polymorphisme Humain (CEPH) family 1345 revealed a functionally heterozygous mother (individual 11). Her son (individual 01) inherited her HSA17 in which CENP-A was located at D17Z1-B and passed it on to at least two of his children (individuals 06 and 07). (*B*) ChIP analysis of CEPH individuals showed equivalent enrichment of CENP-A at D17Z1 and D17Z1-B in individual 11, reflecting differential location on each homolog. In individual 13, CENP-A was enriched at D17Z1, confirming functional homozygosity (CENP-A^{Z1}).

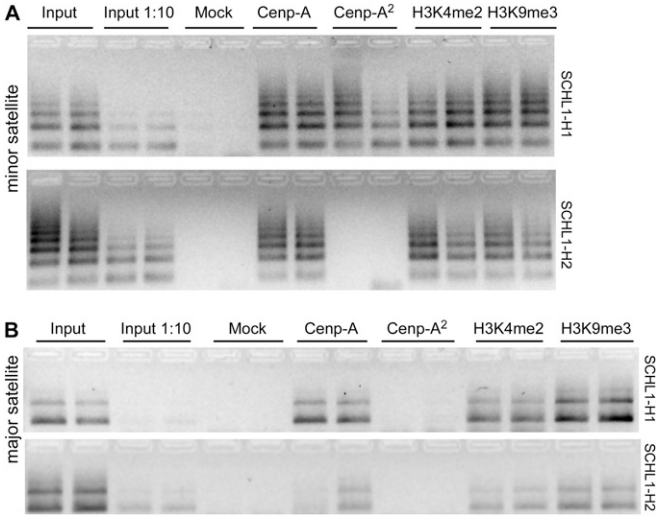

Fig. S3. ChIP data for Cenp-A and histone modifications at mouse minor and major satellite control sites in mouse–human somatic cell hybrids containing single HSA17s. (*A*) Mouse minor satellite sequences in cell lines SCHL1-H1 and SCHL1-H2 (Table S1) were enriched for Cenp-A, H3K4me2, and H3K9me3, as expected. Minor satellite DNA is the site of Cenp-A assembly. (*B*) Mouse major satellite sequences in SCHL1-H1 and SCHL1-H2 were less enriched for Cenp-A and H3K4me2 but were highly enriched for H3K9me3, as expected from previous studies. Lanes 7 and 8 of *A* and *B* represent a custom mouse Cenp-A antibody used for all somatic cell hybrid experiments. Lanes 9 and 10 of *A* and *B* represent a commercial mouse Cenp-A antibody that was only used in initial experiments.

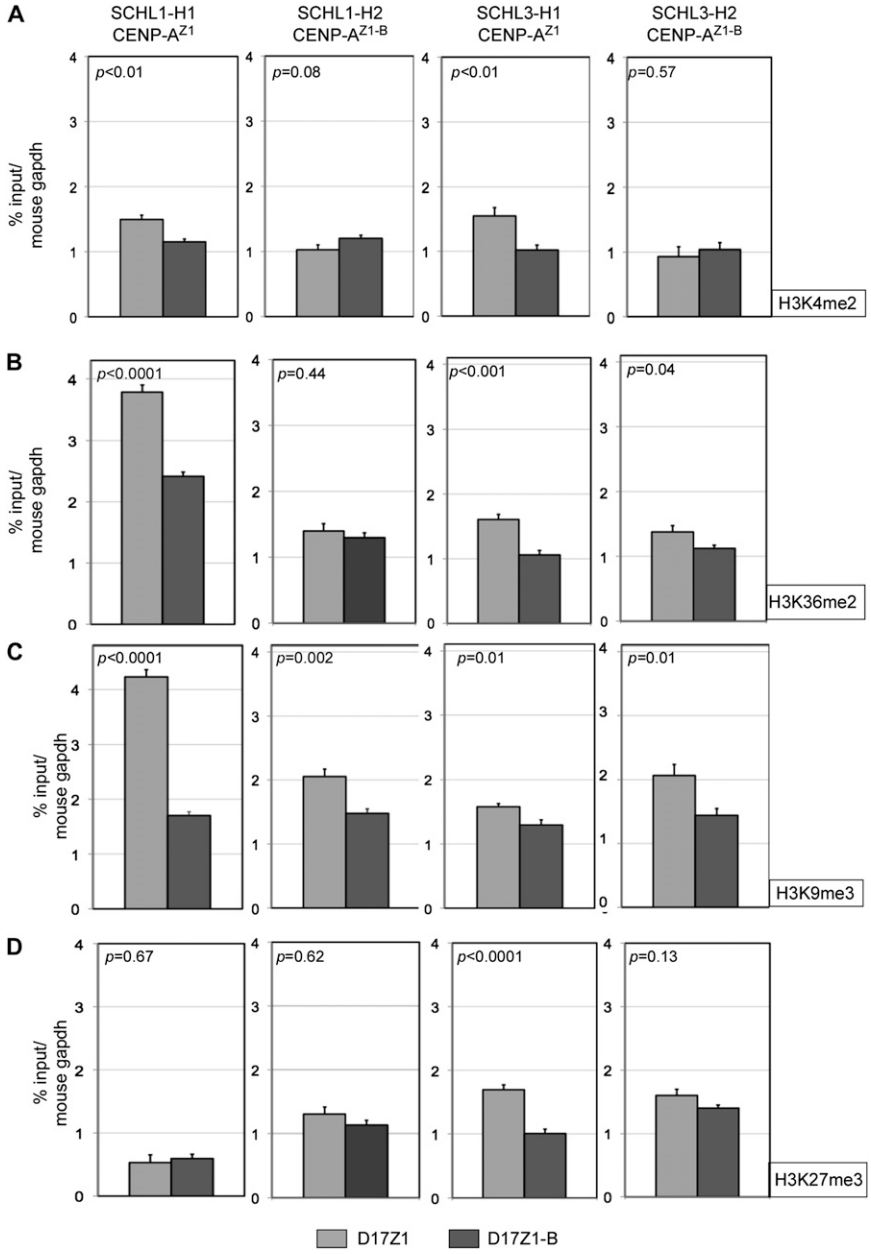

Fig. S4. Heterochromatin profiles of CENP-A–associated and –unassociated HOR arrays on individual HSA17s isolated into somatic cell hybrids. (*A*) Enrichment of H3K4me2 at D17Z1 and D17Z1-B on two HSA17s in which CENP-A is located at D17Z1 or D17Z1-B. Bar graphs represent enrichment from at least two independent ChIPs that contained duplicate or triplicate samples or reactions for each antibody. PCRs were performed in triplicate. Error bars represent SEM. Enrichment is reported as percent input relative to the control site mouse *gapdh*. (*B*) Enrichment for H3K36me2, a euchromatic modification reported to be present within CENP-A–associated chromatin on artificial chromosomes, was enriched at D17Z1 when it was the site of CENP-A assembly. However, when CENP-A was assembled at D17Z1-B, this HOR array was not significantly enriched for H3K36me2 compared with D17Z1. (*C* and *D*) Bar graphs represent enrichment calculated as percent input relative to control mouse *gapdh* from at least two independent ChIPs. PCRs were performed in triplicate for each ChIP. Error bars represent SEM. (*C*) The heterochromatic modification H3K9me3 appeared to be more enriched at D17Z1 than at D17Z1-B, regardless of CENP-A association. Enrichment for histone modification at the target site is reported as percent input relative to mouse *gapdh*. Error bars represent SEM. (*D*) Enrichment for heterochromatic modification H3K27me3 revealed that D17Z1 and D17Z1-B were similarly enriched for H3K27me3 on each HSA17 examined, regardless of which HOR array was the site of CENP-A assembly.

Table S1. Cell lines included in study

Cell line	Cell type	Functional centromeric status*	Source
FIBL1	Colon cancer	Heterozygous	B. Vogelstein (Johns Hopkins University, Baltimore, MD)
FIBL2	Human dermal fibroblast	Homozygous Z1	ATCC
FIBL3	Fibrosarcoma (diploid)	Heterozygous	ATCC
FIBL4	Fibrosarcoma (hypertetraploid)	Heterozygous	ATCC
GM08146	LCL	Homozygous Z1	Coriell
GM08828	LCL	Homozygous Z1	Coriell
GM13019	LCL	Homozygous Z1	Coriell
JK745	LCL	Homozygous Z1	H. Willard (Duke University, Durham, NC)
1345–13	LCL–CEPH	Homozygous Z1	Coriell
1345–11	LCL–CEPH	Heterozygous	Coriell
1345–10	LCL–CEPH	Homozygous Z1	Coriell
1345–02	LCL–CEPH	Homozygous Z1	Coriell
1345–01	LCL–CEPH	Heterozygous	Coriell
1345–06	LCL–CEPH	Heterozygous	Coriell
1345–07	LCL–CEPH	Heterozygous	Coriell
1345–08	LCL–CEPH	Homozygous Z1	Coriell
1345–12	LCL–CEPH	Homozygous Z1	Coriell
1333–02	LCL–CEPH	Homozygous Z1	Coriell
1333–12	LCL–CEPH	Homozygous Z1	Coriell
1333–13	LCL–CEPH	Homozygous Z1	Coriell
1333–01	LCL–CEPH	Homozygous Z1	Coriell
1333–02	LCL–CEPH	Homozygous Z1	Coriell
1333–11	LCL–CEPH	Homozygous Z1	Coriell
1333–13	LCL–CEPH	Homozygous Z1	Coriell
SCHL-13A[†]	Somatic cell hybrid	CENP-A^{Z1}	H. Willard
SCHL-14A[†]	Somatic cell hybrid	CENP-A^{Z1}	H. Willard
SCHL1-H1[‡]	Somatic cell hybrid	CENP-A^{Z1}	This study
SCHL1-H2[‡]	Somatic cell hybrid	CENP-A$^{Z1\text{-}B}$	This study
SCHL3-H1[§]	Somatic cell hybrid	CENP-A^{Z1}	This study
SCHL3-H2[§]	Somatic cell hybrid	CENP-A$^{Z1\text{-}B}$	This study
SCHL-745[¶]	Somatic cell hybrid	CENP-A^{Z1}	H. Willard

All mouse–human somatic cell hybrids were generated using the same L cell/thymidine kinase-deficient mouse cell line. LCL, lymphoblastoid cell line.

*Functional centromere status is defined as homozygous Z1 (both homologs show CENP-A at Z1) or heterozygous (one homolog has CENP-A located at Z1, the other homolog has CENP-A at Z1-B). No homozygous Z1-B (both homologs have CENP-A located at Z1-B) chromosomes have been identified.

[†]Mouse–human somatic cell hybrid containing single HSA17 derived from GM08146.

[‡]Mouse–human hybrid containing single HSA17 derived from FIBL1.

[§]Mouse–human somatic cell hybrid containing single HSA17 from FIBL3.

[¶]Mouse–human somatic cell hybrid containing single HSA17 from JK745.

Table S2. Human artificial chromosome (HAC) results using D17Z1-B constructs

Construct	Cell line	No. cells with HAC (%)	No. cells with integration (%)
RP11-285M22 (145 kb; 18 kb D17Z1-B)*	Z1B.1	1/23 (4)	20/23 (87)
	Z1B.2	0/6 (0)	1/6 (17)
	Z1B.3	3/9 (33)	None
	Z1B.4	1/20 (5)	19/20 (95)
	Z1B.5	0/26 (0)	None
	Z1B.6	1/30 (3)	None
	Z1B.7	0/20 (0)	None
	Z1B.8	0/30 (0)	None
	Z1B.9	0/25 (0)	None
	Z1B.10	2/50 (4)	3/50 (6)
	Z1B.11	0/30 (0)	None
	Z1B.12	0/25 (0)	None
	Z1B.13	0/3 (0)	None
	Z1B.14	1/13 (8)	None
	Z1B.15	2/46 (4)	2/46 (4)
	Z1B.16	0/3 (0)	None
	Z1B.17	0/19 (0)	None
	Z1B.18	0/25 (0)	None
	Z1B.19	0/20 (0)	3/20 (15)
RP11-458D13 (17 kb D17Z1-B)†	1.1	1/11 (9)	None
	1.2	0/20 (0)	None
	1.3	0/19 (0)	None
	1.4	1/18 (6)	None
	1.5	0/11 (0)	None
	1.6	2/19 (11)	None
	2.1	0/7 (0)	None
	2.2	0/10 (0)	None
	2.3	0/9 (0)	None
	2.4	4/9 (44)	None
	2.5	0/10 (0)	None
	2.6	0/10 (0)	None
	2.7	4/10 (40)	None
	2.8	8/10 (80)	None
	2.9	3/4 (75)	None
	2.10	0/7 (0)	None
	2.11	0/6 (0)	None
	2.12	3/10 (30)	None
	2.13	0/8 (0)	None
	2.14	0/10 (0)	None
RP11-285M22Pml (18 kb D17Z1-B)‡	3	9/9 (100)	None
	4	4/11 (36)	None
	5	3/7 (43)	None
	6	0/9 (0)	None
	7	15/21 (71)	None
	8	0/20 (0)	None
	9	9/24 (38)	None
	10	8/23 (35)	None
	11	4/13 (31)	None
	13	9/18 (50)	None
	14	0/8 (0)	None
	15	1/15 (7)	None
	16	6/15 (40)	None
	18	0/12 (0)	None
	20	0/15 (0)	None
	21	8/12 (67)	None
	22	6/7 (86)	None
	23	3/15 (20)	None
	24	1/13 (8)	None

*BAC contained 17 kb of D17Z1-B + 132 kb of monomeric alpha satellite.
†Subcloned BAC contained 17 kb of DXZ1 + 25 kb of monomeric alpha satellite.
‡Subcloned BAC contained 18 kb of D17Z1-B + 30 kb monomeric alpha satellite.

Table S3. HAC results using control alpha-satellite constructs

Construct	Cell line	No. cells with HAC (%)	No. cells with integration (%)
RP11-352P13 (75 kb D17Z1)	Z1.1	0/7 (0)	None
	Z1.2	0/7 (0)	1/7 (14)
	Z1.3	1/23 (4)	None
	Z1.4	2/3 (67)	None
	Z1.5	0/5 (0)	None
	Z1.6	0/35 (0)	None
	Z1.7	1/35 (3)	1/35 (3)
	Z1.8	0/29 (0)	None
	Z1.9	0/29 (0)	None
	Z1.10	0/20 (0)	None
RP11-971O21SwaI (16 kb DXZ1)	2	2/6 (33)	None
	4	0/17 (0)	None
	5	0/13 (0)	None
	6	0/16 (0)	None
	8	5/15 (33)	None
	9	1/17 (6)	None
	15	0/18 (0)	None
	18	5/15 (33)	None
	22	0/16 (0)	None

Table S4. Primers used for PCR

Name	Forward	Reverse
Kan/Neo	TCAGGAATTCAGGGAAGAAAGCGAAAGGAG	ATGCGGTACCACGCTCAGTGGAACGAAAAC
FW1/RV1	TAGTCAATTCGGGAGGATCG	GCGCTGGAGAATAGGTGAAG
FW2/RV2	CGGGTTATTTTCCTCGCTTCC	AATGTCAAGCTCGACCGATG
D17Z1 (q/SQ-PCR)	AAAACTGCGCTCTCAAAAGG	AATTTCAGCTGACTAAACA
D17Z1-B (q-PCR)	ACTTTCTGTAGAATCTGCG	CTAGATTTTATTTGAAGATGTA
D17Z1-B (SQ-PCR)	ACTTTCTGTAGAACTTGCG	TCA TCT GCT CTA TGA AT
5s rDNA human	CCGGACCCCAAAGGCGCACGCTGG	TGGCTGGCGTCTGTGGCACCCGCT
5s rDNA mouse	CCTGTGAATTCTCTGAACTC	CCTAAACTGCTGACAGGGTG
pRetroES-*lox*P	ATCGACCGGTAATGCAGGCA	TCAGCGTGAGACTACGATTC
pRetroES-*lox*511	ATCGACCGGTAATGCAGGCA	GTTGCTACGCCTGAATAAGTG
D17S2040	TCTTATTGCATGAGTCCAAGC	TCTTTTGGCTGTAAGGAACG
SLC6A4 (intron 2 VNTR)	GGGCAATGTCTGGCGCTTCCCCTACATA	TTCTGGCCTCTCAAGAGGACCTAGAGG

qPCR, quantitative PCR; SQ-PCR, semiquantitative PCR.